Supplemental figure legends

Supplemental_Figure_S1. *Density gradient centrifugation allows separation of mature sperm and spermatids.*

Microscopic observations with DAPI staining confirm that sperm and spermatids have been successfully separated based on morphological differences: **(A)** Mature sperm in *Xenopus laevis* have a characteristic snake-like shape, which allows their easy discrimination from other cell types (Risley 1979; Risley et al. 1982). **(B)** spermatids have round nuclei resembling somatic cells. **(C)** FACS analysis on propidium iodide-stained spermatid cell population confirmed that 79.32% cells were haploid and the remaining 20% consisted of diploid and tetraploid testicular cells.

Supplemental_Figure_S2: *Embryos generated following fertilisation of UV enucleated eggs are haploid.*

Eggs were subjected to 30s Mineralite UV lamp treatment for enucleation and subsequently fertilised (Gurdon 1962) . Control eggs were directly fertilised, omitting the Mineralite treatment. **(A)** Microscopic observations of control embryos (non-enucleated) (left panel, 'diploid embryos') and of embryos obtained from Mineralite-treated eggs (enucleated) (right panel, 'haploid, enucleated embryos') reveals that haploid embryos are vegetalised and therefore confirms the successful egg enucleation. Note that the vegetalised phenotype is not apparent at the gastrula stage (upper panel) and only becomes visible when the embryo elongates (bottom panel). Scale bars = 1mm. **(B)** Microscopic observations of cells from control embryos (left panel) and from embryos obtained from Mineralite-treated eggs (right panel) confirms

a successful egg enucleation. Note that in the nuclei of cells from diploid embryos two nucleoli (black dots) are visible (left panel), whereas in the nuclei of cells from haploid embryos only one nucleolus per nucleus can be detected (single black dots). Examples of nuclei in each cell preparation are inside the red circles. The presence of two or one nucleoli per nucleus is indicative of the diploid or haploid nature of the embryos (Elsdale et al. 1958) .

Supplemental_Figure_S3: *RNA carry-over is not the cause of developmental defects of spermatid-derived embryos*

Fertilised embryos (at 1-cell stage) were injected either with water, with 50pg of mRNAs encoding sperm basic proteins (Sp1, Sp4 and Sp5) or with 50pg of total testicular RNA ('Total RNA', obtained by TRIzol purification). Injections did not affect the normality of embryonic development, since all embryos developed into normal swimming tadpoles.

Supplemental_Figure_S4: *Spermatid-derived embryos are as good as sperm-derived embryos at synthesising rRNAs.*

(A) Diagram explaining newly synthesised RNA isolation from sperm- and spermatid-embryos. Haploid sperm- and spermatid-embryos are obtained by ICSI to enucleated eggs and are co-injected with BrUTP to label newly synthesised RNA. Once embryos reach gastrula stage they are collected and BrUTP-labelled, newly synthesised RNAs are pulled down. **(B)** Spermatid-derived embryos synthesise rRNA as efficiently as sperm-derived embryos, as evidenced by RT-qPCR quantification of

18S and 28S rRNAs. Values are shown as a percentage of pulled down RNA to the total input RNA. Error bars show ± sem. N=20 sperm-derived embryos and N=14 spermatid-derived embryos. Samples were not significantly different (p-value = 0.82 for 18S rRNA and p-value = 0.36 for 28S rRNA, t-test).

Supplemental_Figure_S5: *Sperm and spermatid mononucleosomal fraction obtained by MNase digestion.*

Chromatin isolated from 1 million of sperm, spermatids or XL177 cells was digested with 2.5 units of MNase for 30mins at 37ºC. Subsequently, DNA was isolated and run on a 1.6% agarose gel. Spermatids and XL177 cells digestion pattern displays a typical 'nucleosome ladder' (mononucleosome band size indicated), whereas digestion of sperm revealed a unique structure of sperm chromatin, consisting of three bands of approximately 150bp, 110bp and 75bp (bands are respectively numbered 1, 2, 3 and indicated on the gel). The lowest band (4) is digested DNA, which was also observed when mouse or human sperm is digested with MNase (Brykczynska et al. 2010).

Supplemental_Figure_S6: *Nucleosome occupancy at TSS in sperm and spermatid chromatin for genes differentially expressed in spermatid-derived embryos compared to sperm-derived embryos.*

Average nucleosome occupancy patterns in sperm (A) and in spermatid (B) in the 2kb window centred around TSS of genes that are upregulated in spermatid-derived embryos. (C) Weighted fraction of estimated nucleosome positions in different

genomic features for sperm and spermatid. Nucleosome occupancy and nucleosome positions were estimated as described in *Supplemental experimental procedures*.

Supplemental_Figure_S7: *DNA methylation levels of genes differentially expressed in spermatid-derived embryos compared to sperm-derived embryos are similar in sperm and spermatid chromatin.*

Box-plot showing DNA methylation levels in sperm (blue) and spermatid (green) in the 2kb window around TSS of genes misregulated in spermatid-derived haploid embryos. p-value represents the difference between the two distributions (KS-test). Inset scatter plot shows correlation of DNA methylation levels between sperm and spermatid ($R = 0.672$, p-value < 0.05); red line: linear regression; grey line: diagonal.

Supplemental_Figure_S8. *Empirical Cumulative distribution curves (ECDF) for H3K27me3, H3K4me3, H3K4me2 and H3K9me3 in sperm and in spermatids.*

Columns show ECDFs of histone methylation levels for all the marks screened (H3K27me3, H3K4me3, H3K4me2, H3K9me3). Panels in the first row show methylation levels of misregulated genes *versus* genome-wide levels in sperm. The second row shows the same for spermatids. The third row shows sperm versus spermatids ECDFs at misregulated genes only. In each panel statistical significance of the difference between ECDFs is indicated (p-value from KS-test (see also Supplemental Table S5)).

Supplemental_Figure_S9: *H3K27me3 target genes that lose H3K4me2/3 in sperm compared to spermatids are misregulated in spermatid-derived embryos.*

(A, B) Differential gene expression between sperm- and spermatid-derived embryos best correlates with differential H3K4me2/3 and H3K27me3 marking in sperm and spermatid. Partial correlation network between all tested epigenetic features of the paternal chromatin (**A**- sperm, **B**- spermatid) and gene expression in the corresponding embryos. Edges represent positive (red) or negative (blue) partial correlations. Edges thickness: strength of the partial correlations. To increase the predictive power of the analysis an extended set of genes was used by relaxing the selection parameters from FDR≤ 0.05 (255 genes used in figure 5 A&B, 80% of these genes are upregulated in spermatid-derived embryos) to FDR ≤ 0.4 and |logFC| ≥ 0.2 (1116 genes, 66% of these genes are upregulated in spermatid-derived embryos)).

Supplemental_Figure_S10: *Histone demethylases specifically remove target histone modification from sperm and embryonic chromatin.*

(A) H3K27me3 is removed from sperm chromatin transplanted to oocytes overexpressing KDM6B. Sperm nuclei were injected to the germinal vesicle of control or KDM6B expressing oocytes. 3h after injection germinal vesicles were manually dissected, fixed, and immunolabelled with antibodies against H3K9me2/3 and against H3K27me3. Confocal analysis shows that within 3 hours after injection, H3K27me3 is removed from the sperm chromatin whereas H3K9me3 is unchanged. This indicates that KDM6B can rapidly and specifically erase H3K27me3 from sperm chromatin injected to oocytes. **(B)** *In vitro* fertilized embryos were collected 2 days after injection of control or *Kdm6b* mRNAs. Western blot analysis indicates

thatKDM6B demethylates H3K27me3 in embryos without affecting the level of H3K9me2/3 and H3K4me3. **(C)** H3K27me3 demethylase overexpression in immature oocytes leads to decreased levels of H3K27me2/3 in the corresponding IVM/ICSI embryos. **(D)** H3K4me2/3 demethylase overexpression in immature oocytes leads to decreased levels of H3K4me2/3 in the corresponding IVM/ICSI embryos. H3K9me2/3 level are unchanged by KDM5B expression.

Supplemental_Figure_1

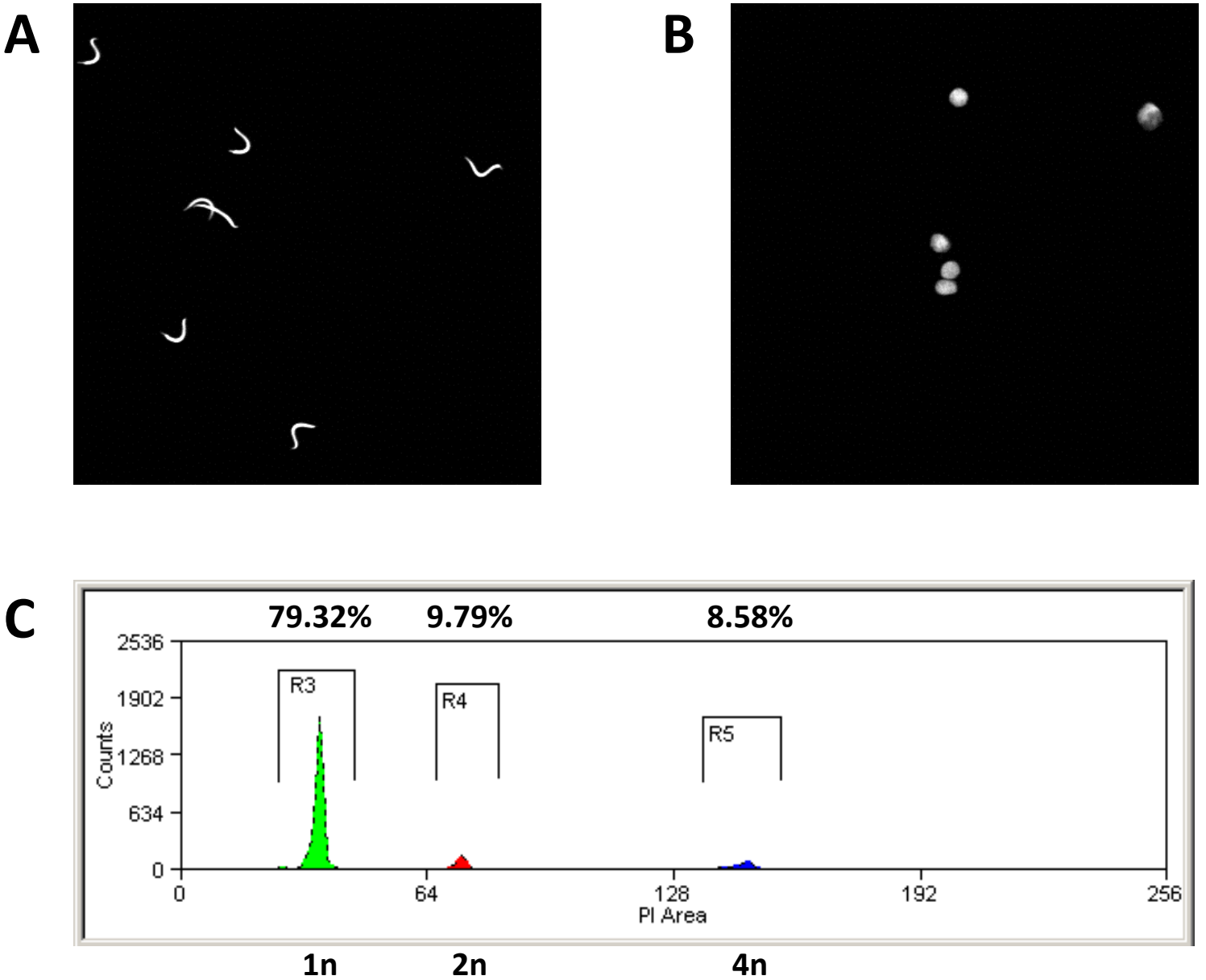

Supplemental_figure_2

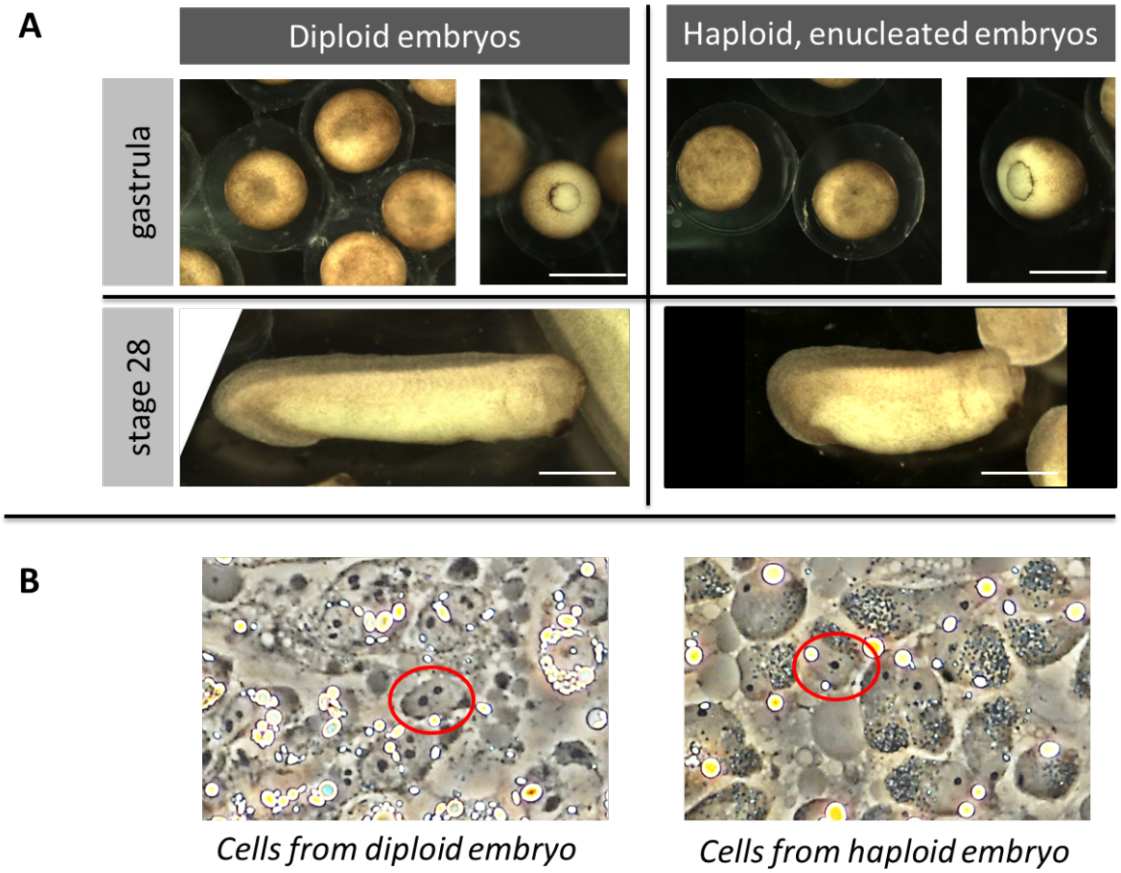

Supplemental_Figure_3.

Supplemental_Figure_4

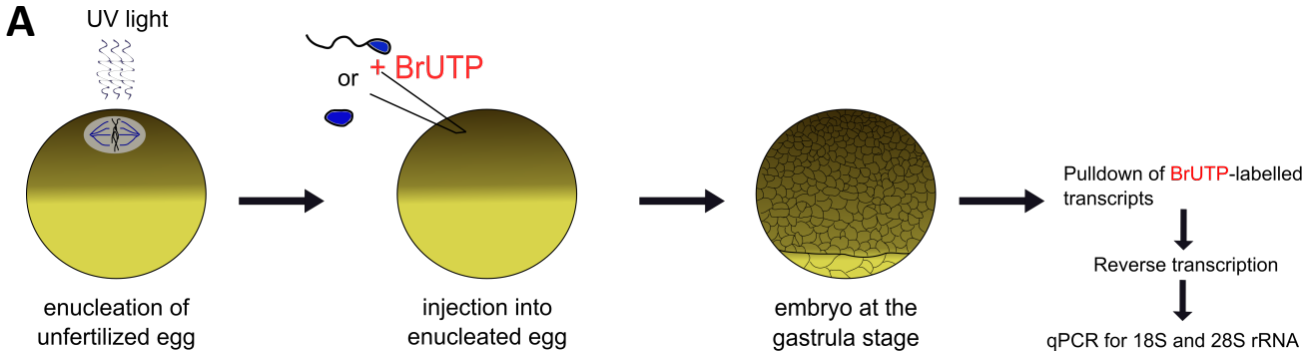

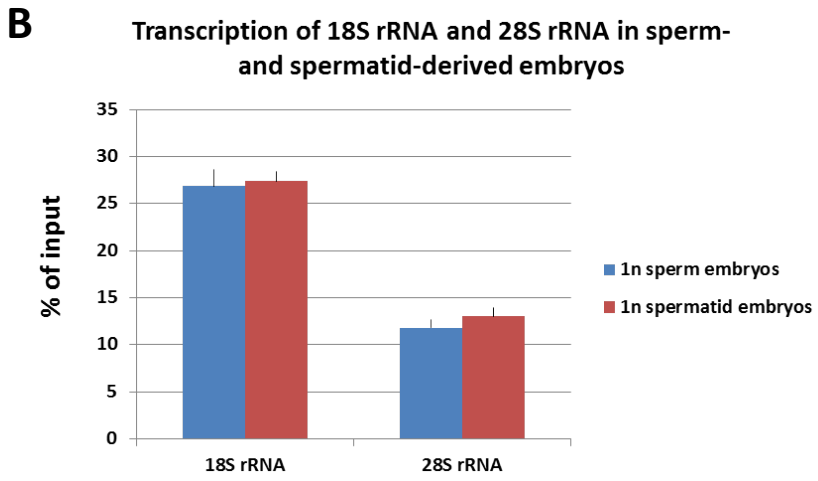

Supplemental_Figure_5

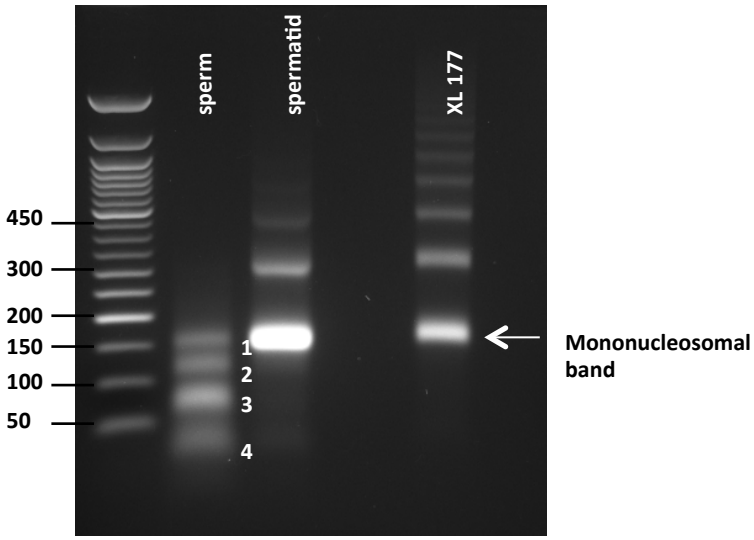

Supplemental_Figure_6

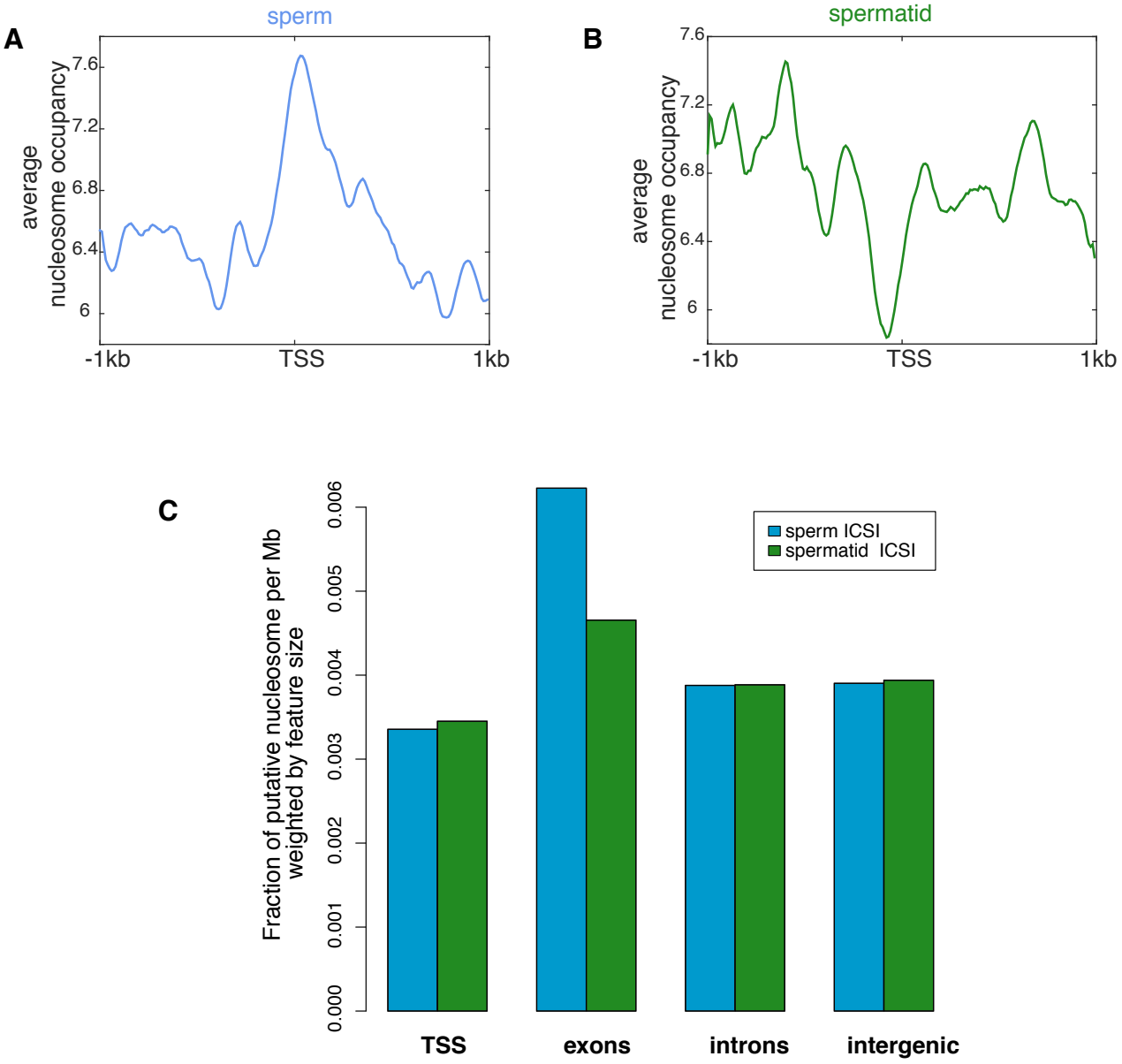

Supplemental_Figure_7

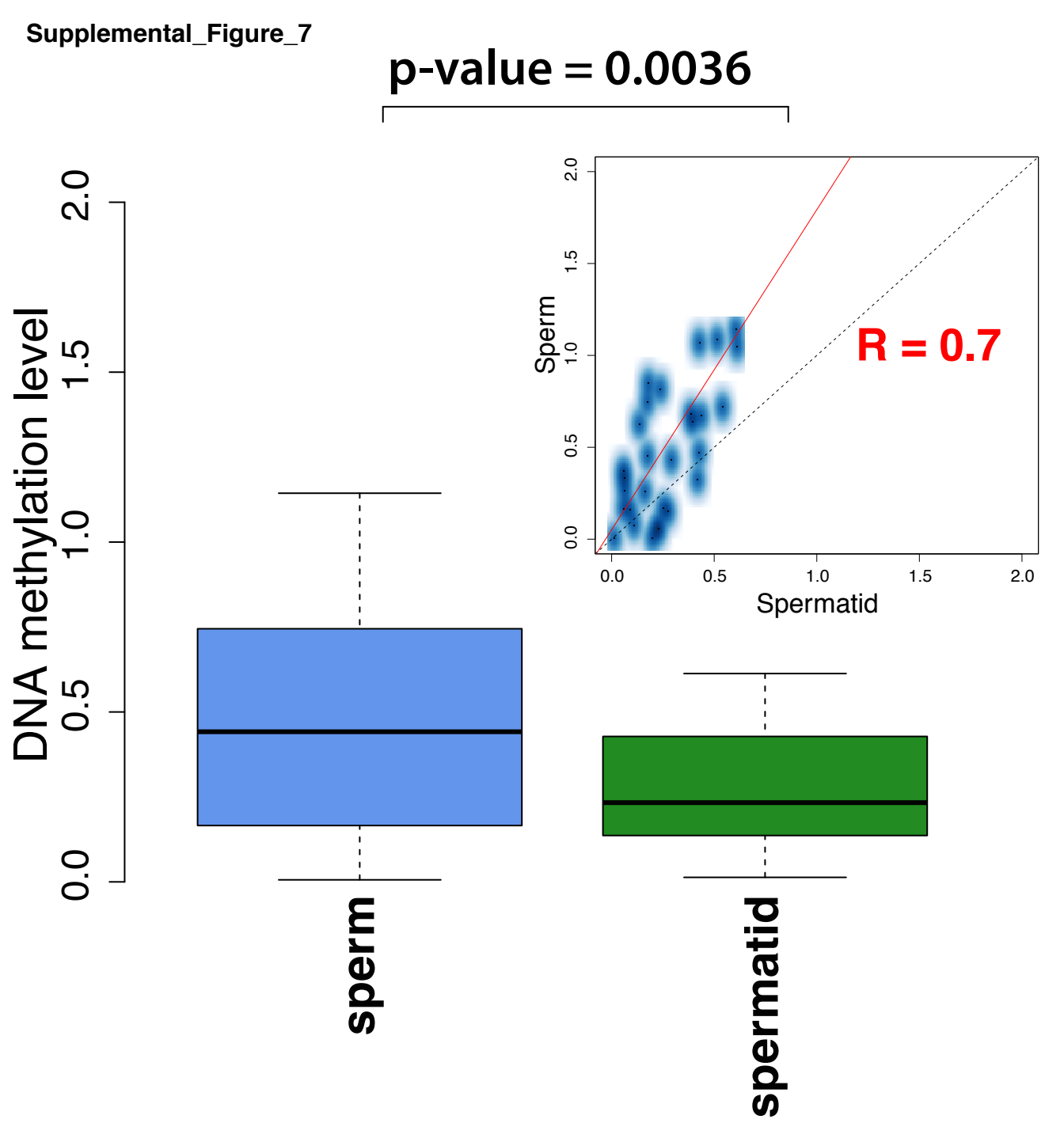

Supplemental_Figure_8

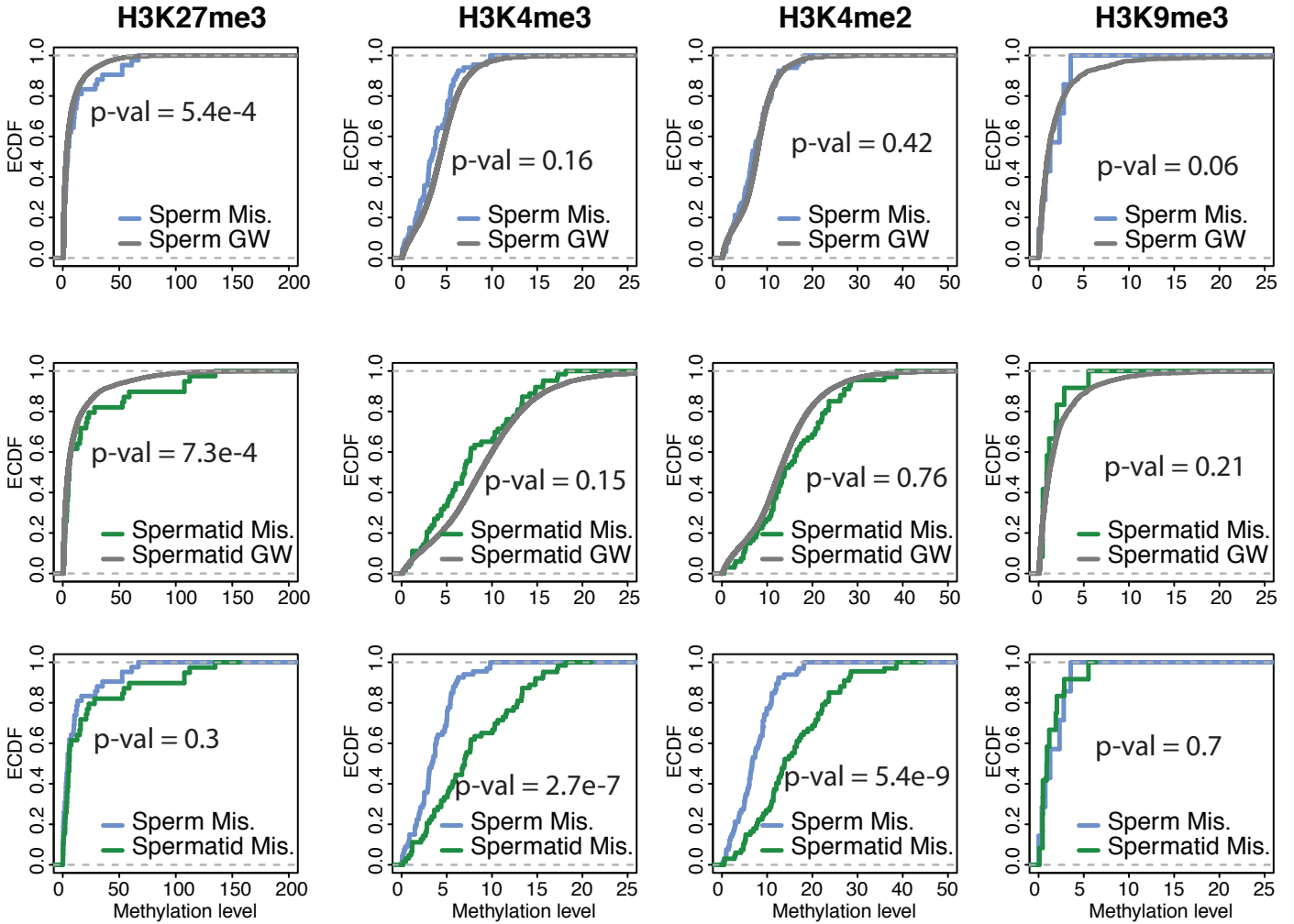

Supplemental_Figure_9

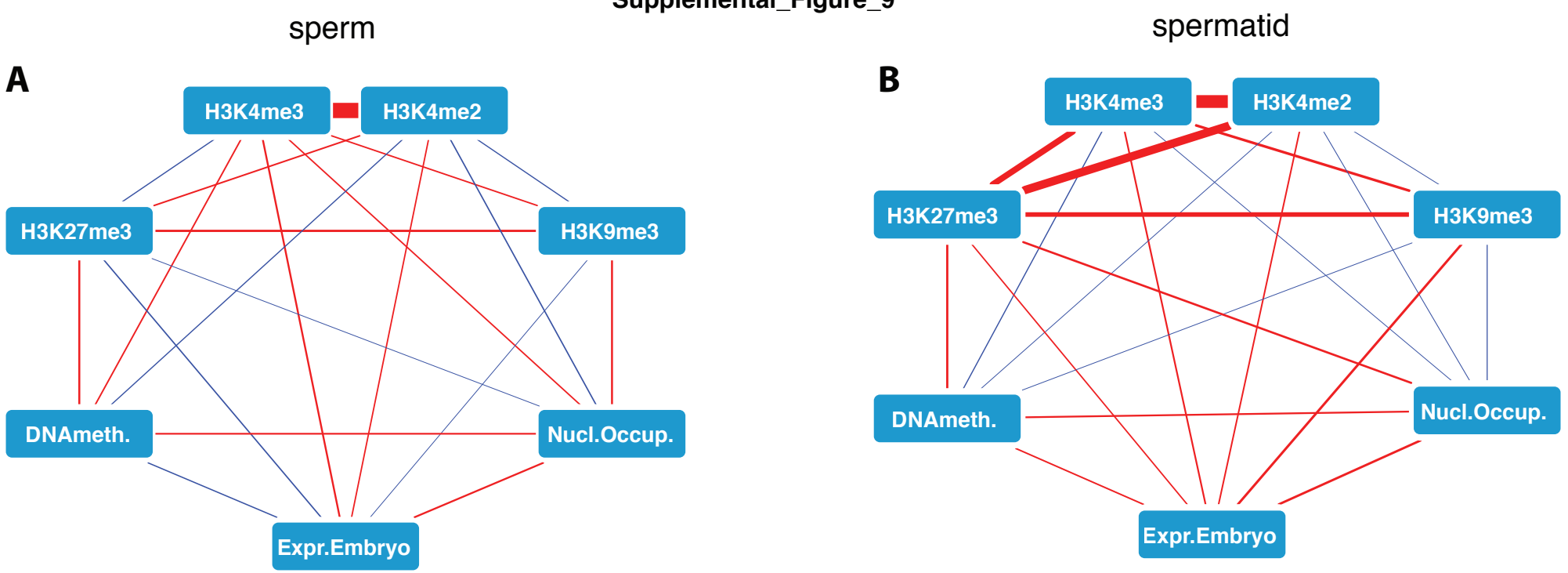

Supplemental-Figure_10